coatings

MDPI

Article

Supplementary Materials: Nanoscale Correlations of Ice Adhesion Strength and Water Contact Angle

Sigrid Rønneberg [1,2], Senbo Xiao [1], Jianying He [1] and Zhiliang Zhang [1,*]

[1] NTNU Nanomechanical Lab, Department of Structural Engineering, Norwegian University of Science and Technology (NTNU), Richard Birkelandsvei 1A, NO-7491, Trondheim, Norway

[2] Justervesenet—Norwegian Metrology Service, Fetveien 99, 2007 Kjeller, Norway

* Correspondence: zhiliang.zhang@ntnu.no

The supplementary materials include 2 tables and 11 figures, as specified below.

Type of system	Mean value for ε_0 [MPa]	SD
System A	486.92	22.106
System B	464.78	21.529
System C	485.532	9.159
System D	452.774	37.642
$k_B = 500\,\mathrm{kJmol^{-1}nm^{-2}}$	406.61	–
$k_B = 3000\,\mathrm{kJmol^{-1}nm^{-2}}$	489.20	15.136
$k_B = 4000\,\mathrm{kJmol^{-1}nm^{-2}}$	470.38	23.967
$k_B = 5000\,\mathrm{kJmol^{-1}nm^{-2}}$	482.66	13.908
$k_B = 6000\,\mathrm{kJmol^{-1}nm^{-2}}$	477.82	36.421
$k_B = 7000\,\mathrm{kJmol^{-1}nm^{-2}}$	468.13	13.004
Xiao et al [39]	259	21

Table S1. Mean value and standard deviation for ice adhesion strength of simulation systems with different sizes and spring constants, all reported for original interaction energy ε. Systems A and B were run with spring constants $k_B = 5000\,\mathrm{kJmol^{-1}nm^{-2}}$, while systems C and D were run with spring constants $10\,000\,\mathrm{kJmol^{-1}nm^{-2}}$. The different spring constants were tested with simulation system A. The value from Xiao et al [39] are from an analogous system with similar parameters.

ε	System A	System B	System C	System D
$0.05\varepsilon_0$	$121.44° \pm 5.12°$	$117.38° \pm 8.50°$	$134.76° \pm 9.68°$	$125.46° \pm 12.05°$
$0.1\varepsilon_0$	$113.74° \pm 1.91°$	$111.37° \pm 3.13°$	$122.95° \pm 7.94°$	$133.22° \pm 17.00°$
$0.5\varepsilon_0$	$91.94° \pm 4.65°$	$89.33° \pm 7.53°$	$93.15° \pm 4.36°$	$96.33° \pm 2.98°$
ε_0	$73.49° \pm 3.44°$	$64.49° \pm 2.42°$	$79.65° \pm 4.19°$	$91.46° \pm 6.21°$
$1.5\varepsilon_0$	$54.51° \pm 2.01°$	$61.58° \pm 24.15°$	$70.34° \pm 8.47°$	$66.81° \pm 8.25°$
$2\varepsilon_0$	$37.00° \pm 2.23°$	–	$43.39° \pm 1.01°$	$51.39° \pm 7.22°$
$2.5\varepsilon_0$	$21.79° \pm 8.51°$	–	$17.23° \pm 2.47°$	$40.07° \pm 11.07°$

Table S2. Mean contact angles and standard deviations for the four different systems and the different interaction energies, as defined in Table 1.

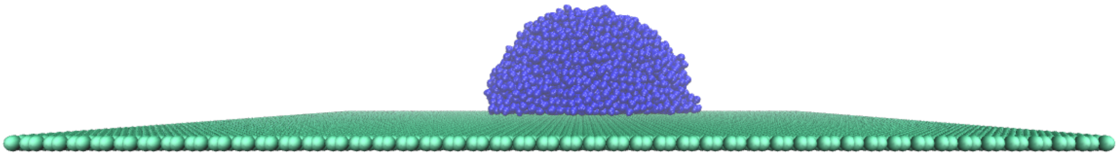

(a) System A.

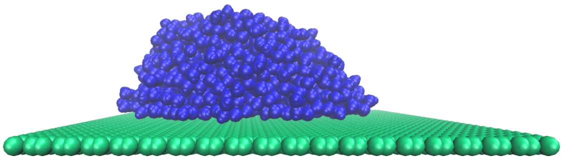

(b) System B.

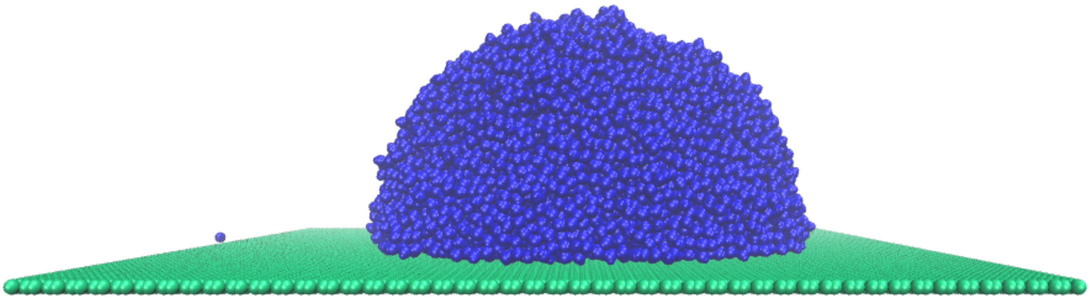

(c) System C.

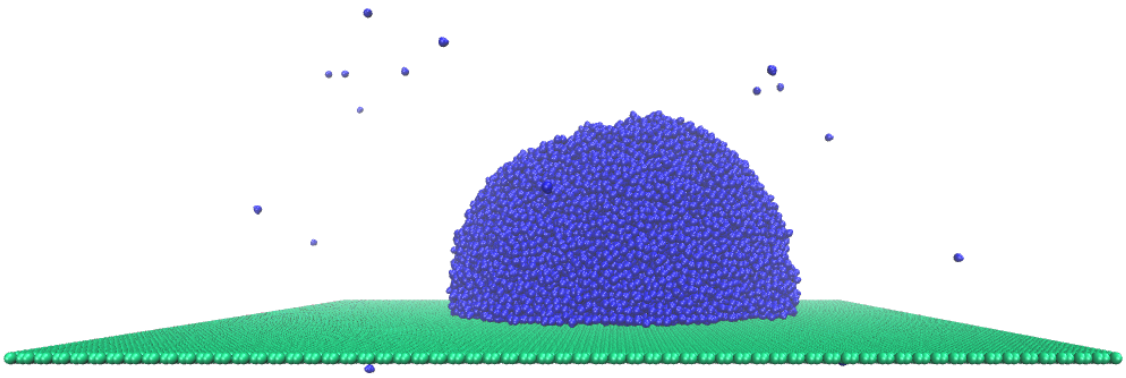

(d) System D.

Figure S1. The four simulation systems from Table 2 with equilibrated water droplets.

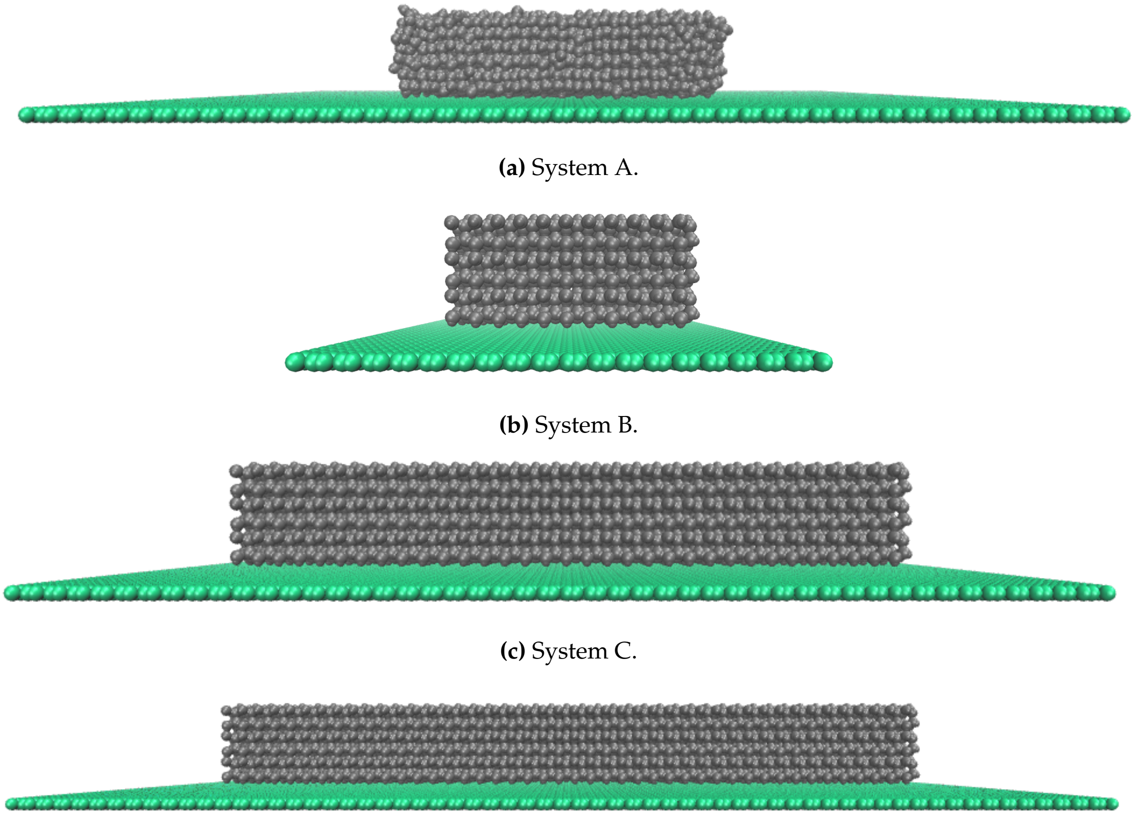

(a) System A.

(b) System B.

(c) System C.

(d) System D.

Figure S2. The four simulation systems from Table 2 with ice samples before detachment.

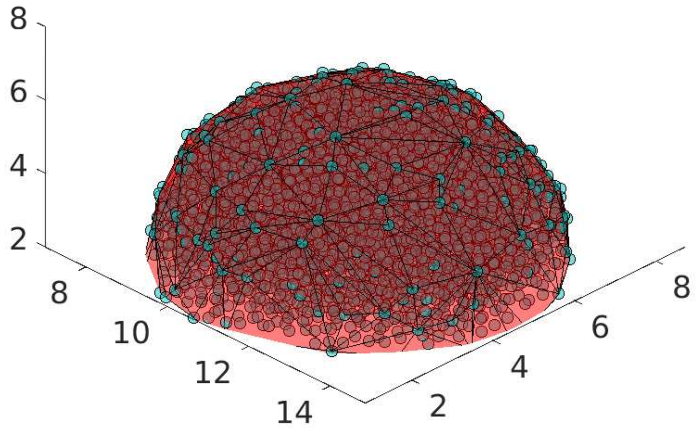

Figure S3. Illustration of the quickhull-algorithm for mapping the droplet, as performed in this study and developed by Khalkhali et al [64]. The imaged droplet is for the normal sized system and original energy well depth ε_0 in Table 1.

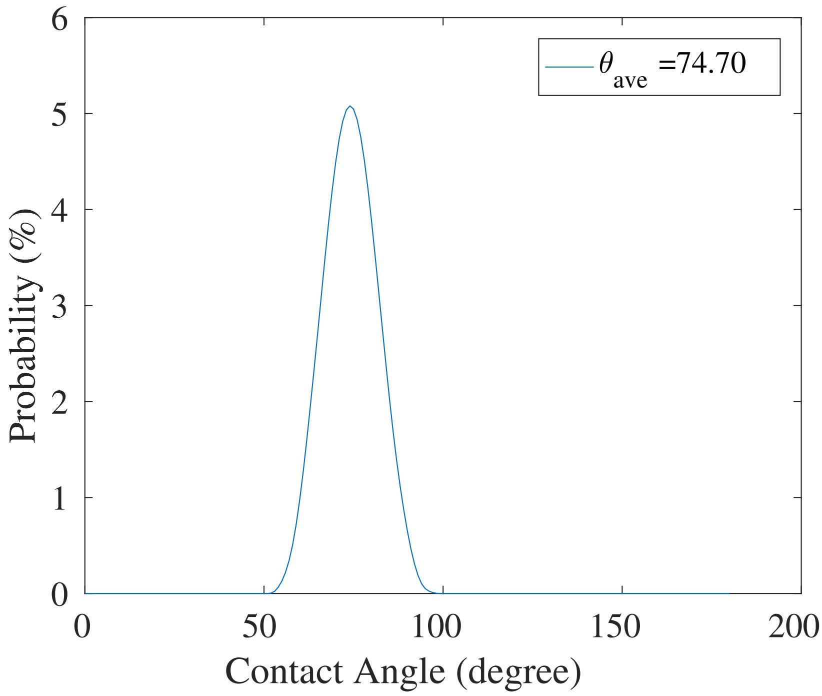

Figure S4. Illustration of the contact angle probability distribution, as performed in this study and developed by Khalkhali et al [64], with the average value indicated. The contact angle distribution is for the droplet imaged in Figure S3, for system A and energy well depth ε_0 in Table 1.

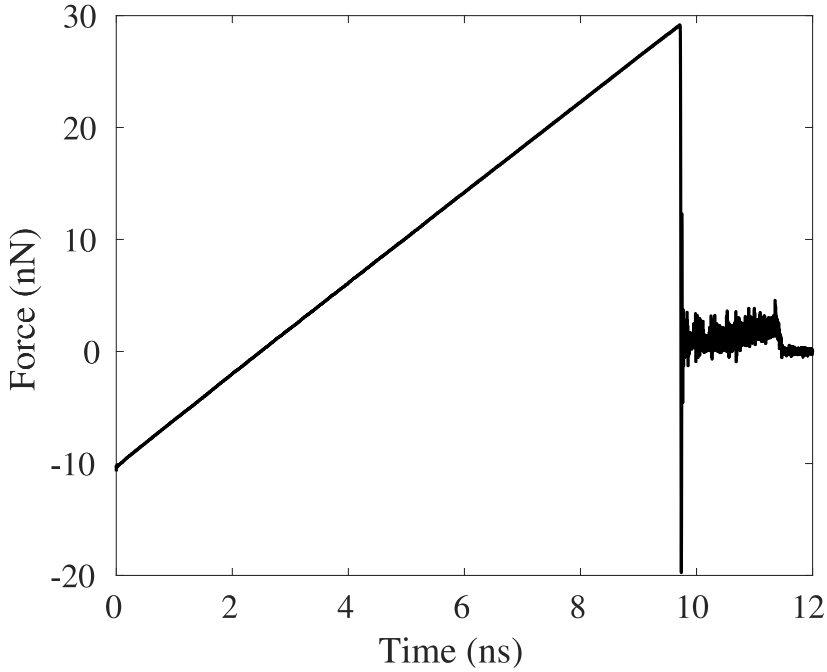

Figure S5. The resulting force-time curve when detaching an ice cube from the graphene surface to calculate the ice detachment stress, which is given by the first force maxima and dividing by the ice-solid area. The curve is for the ice cube analogous to the water droplet imaged in Figure S3, for the normal sized system and original energy well depth ε_0 in Table 1.

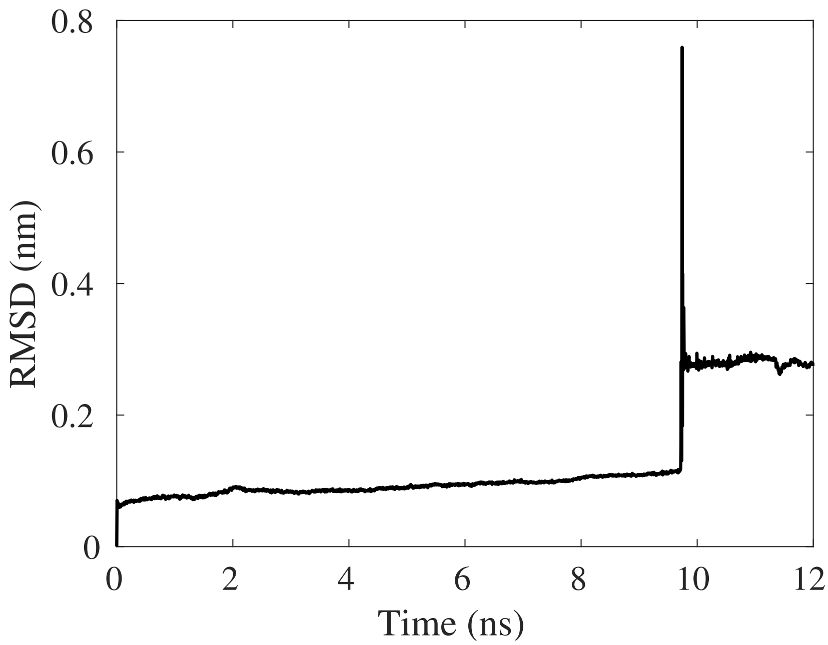

Figure S6. Root mean square deviation (RMSD) of ice for the ice detachment process with force curve in Figure S5. Even though the force from the harmonic oscillator presses the ice into the graphene surface at the start of the simulation, as seen by the negative force, the RMSD shows that the ice is not impacted by this pressing movement before it is pulled away from the graphene surface.

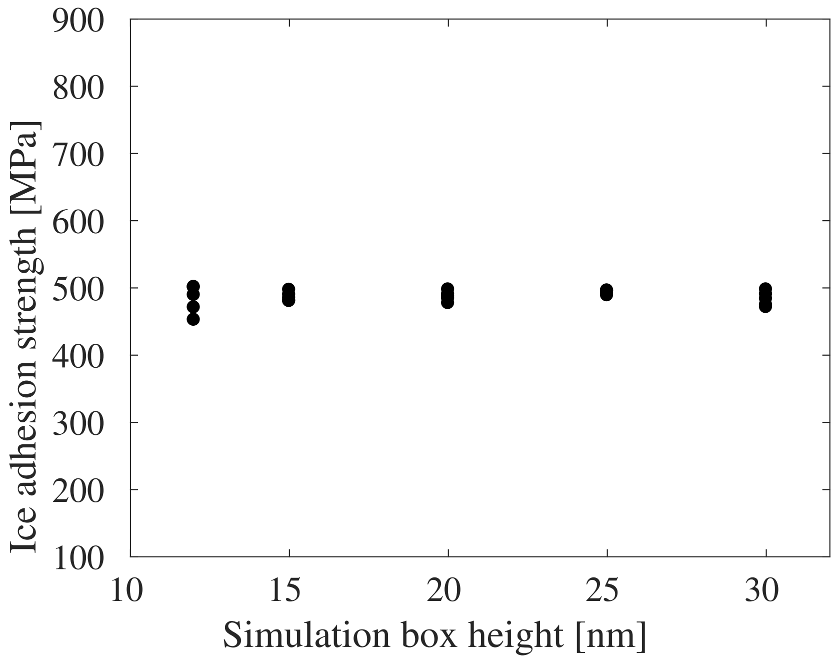

(a) Effect of changing box size in z-dimension.

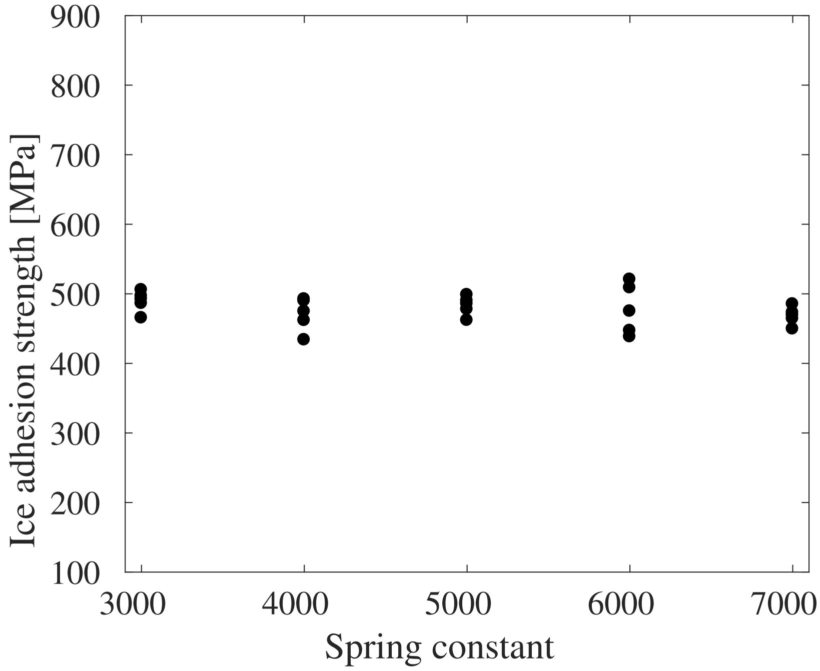

(b) Effect of changing spring constant in pulling.

Figure S7. Effect of changing simulation parameters on the recorded ice adhesion strength. Simulations performed for normal system. Parameters utilized in the simulations otherwise were spring constant $k_B = 5000\,\mathrm{kJmol^{-1}nm^{-2}}$ and box size 12 nm.

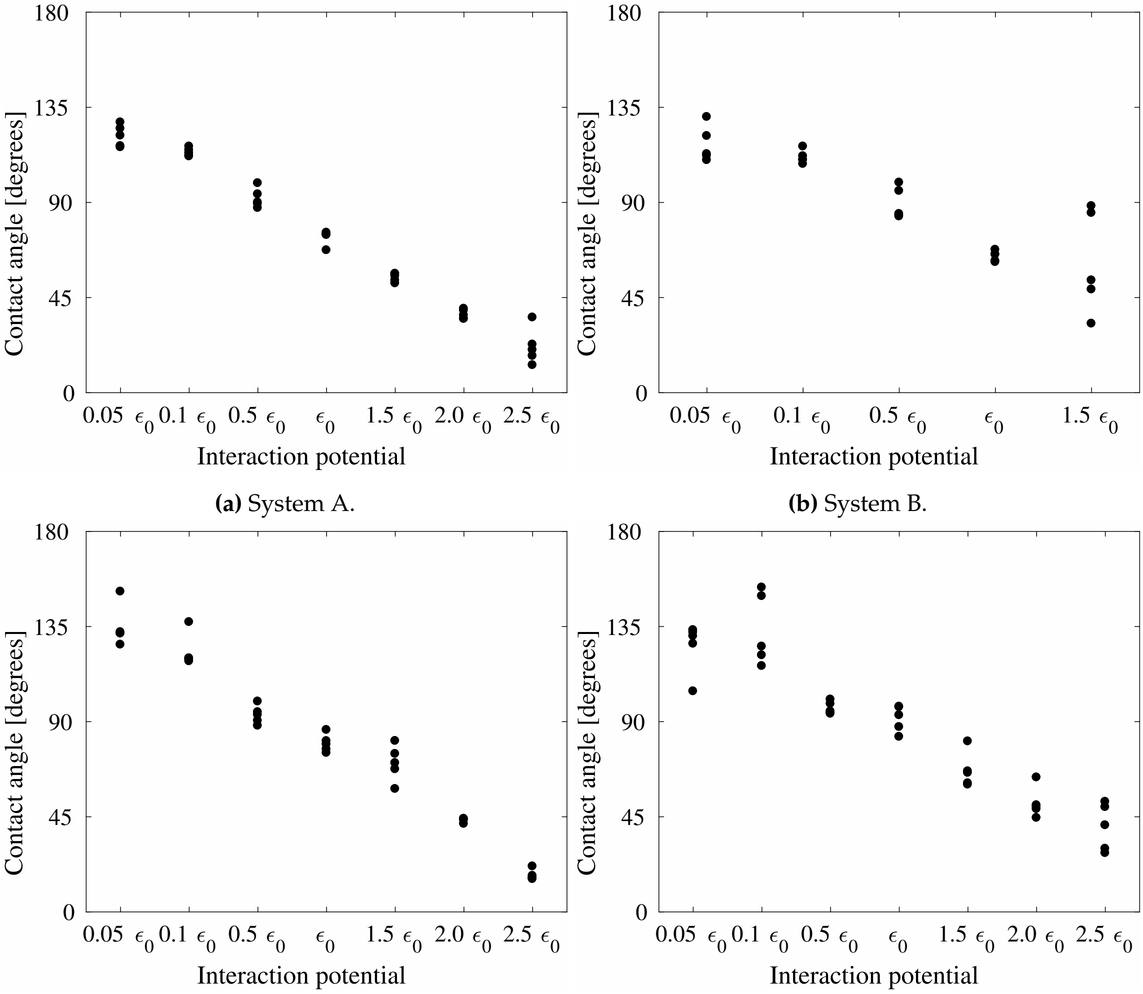

(a) System A.

(b) System B.

(c) System C.

(d) System D.

Figure S8. Contact angle as function of interaction potential ε for the four different system sizes.

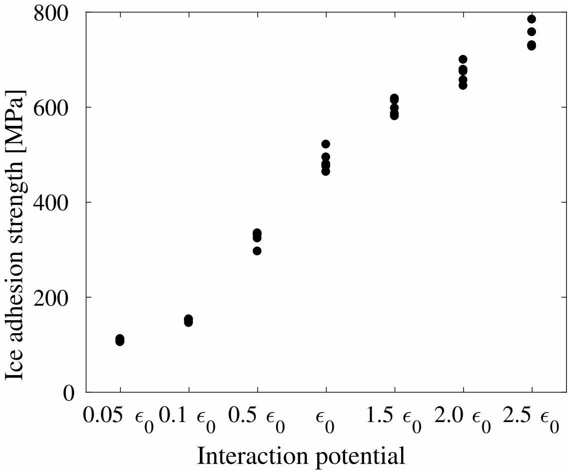

(a) System A.

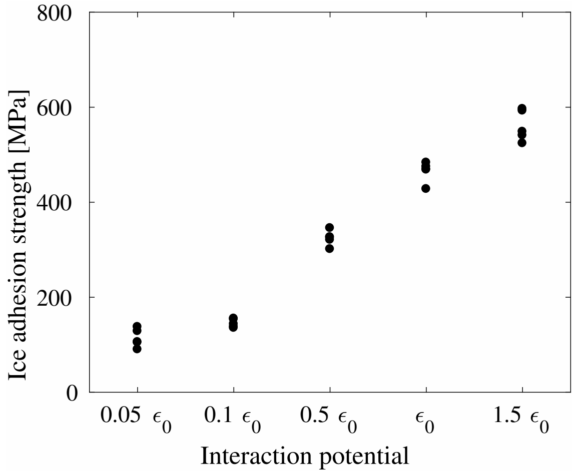

(b) System B.

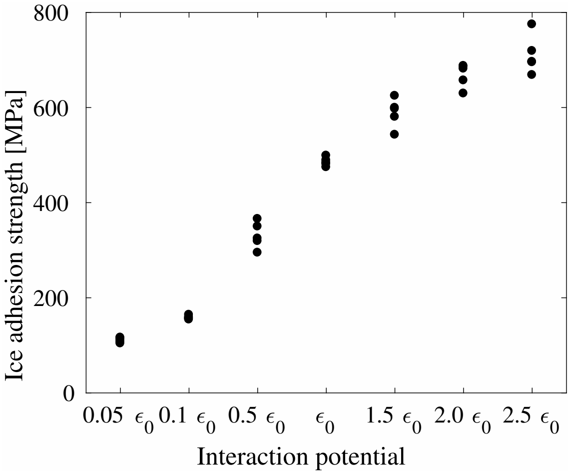

(c) System C.

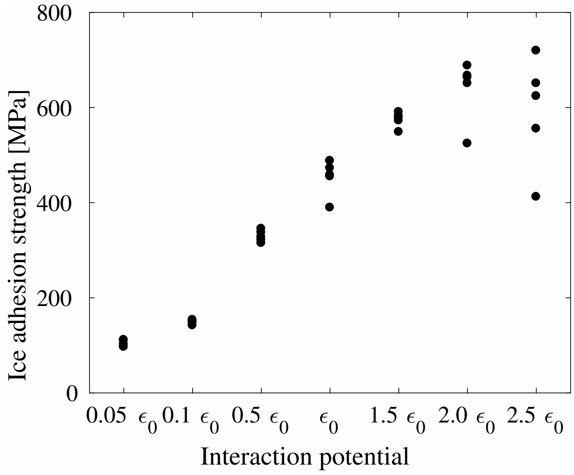

(d) System D.

Figure S9. Ice adhesion strength as function of interaction potential ε for the four different system sizes.

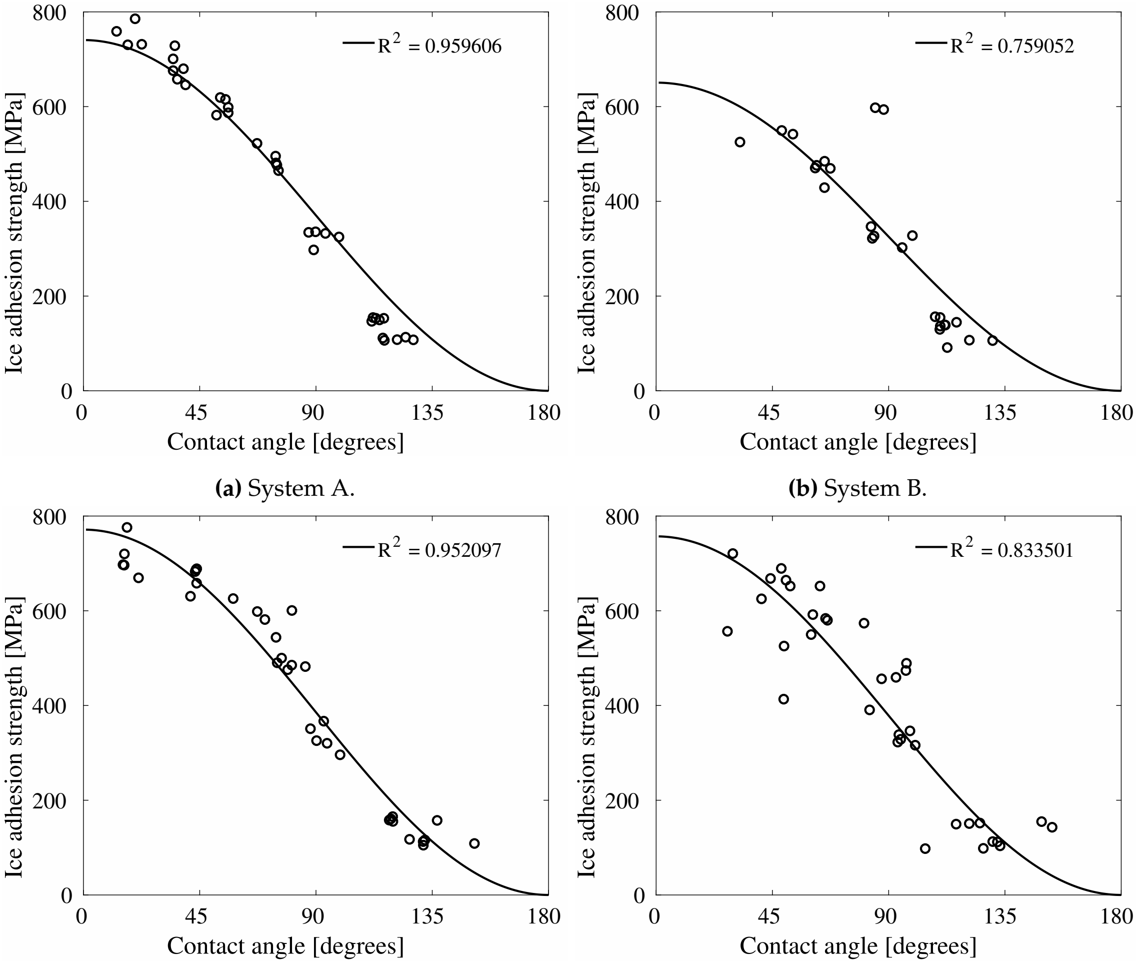

(a) System A.

(b) System B.

(c) System C.

(d) System D.

Figure S10. Ice adhesion strength as function of contact angle with fitting from equation (7) for the four different system sizes.

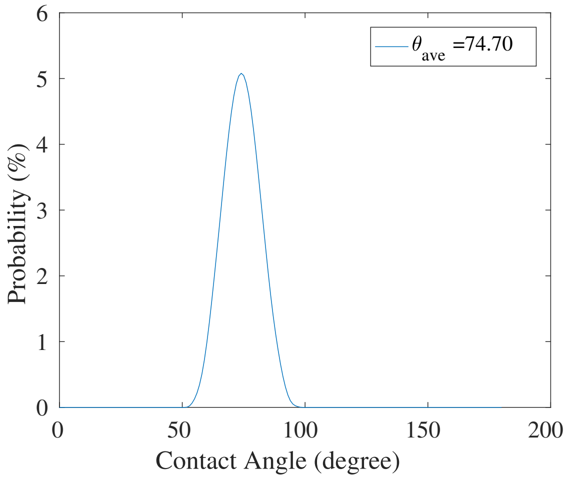

(a) System A.

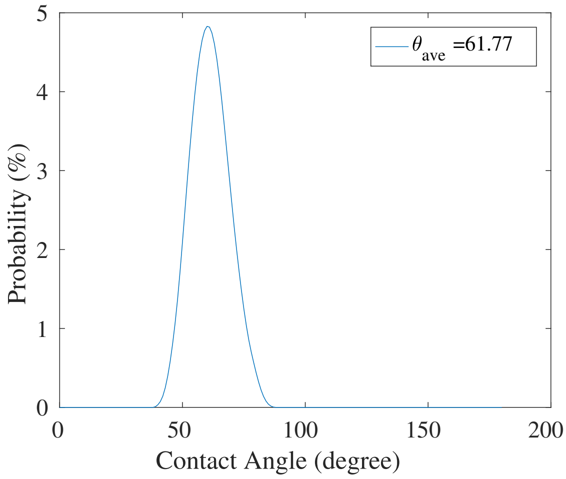

(b) System B.

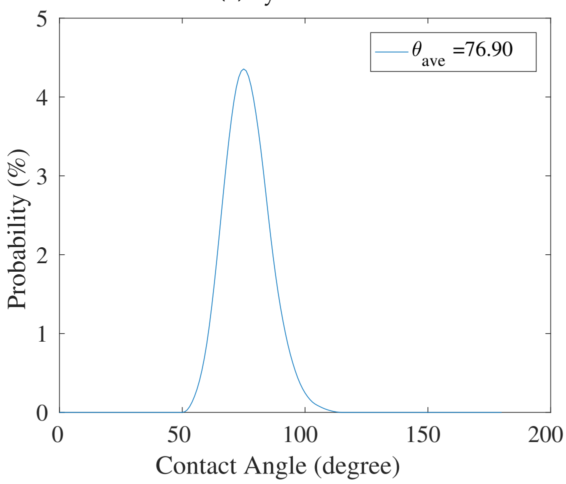

(c) System C.

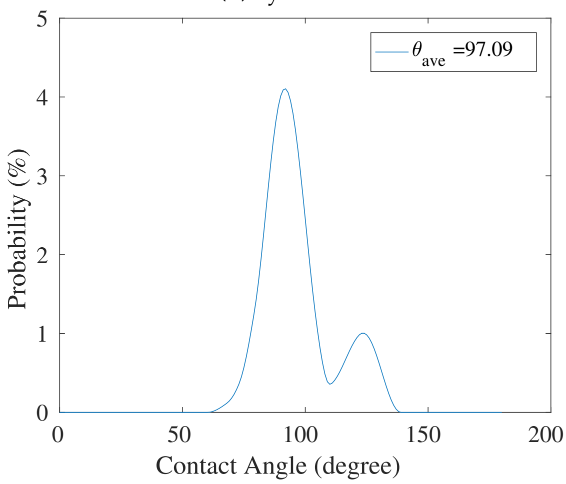

(d) System D.

Figure S11. Contact angle distributions for the first simulations performed with interaction energy ε_0 for the four different system sizes.

References

39. Xiao, S.; He, J.; Zhang, Z. Nanoscale deicing by molecular dynamics simulation. *Nanoscale* **2016**, *8*, 14625.
64. Khalkhali, M.; Kazemi, N.; Zhang, H.; Liu, Q. Wetting at the nanoscale: A molecular dynamics study. *J. Chem. Phys.* **2017**, *146*, 114704.